Problem Set 5 (**Due February 25th**)

1. Show how glucose can be converted to two equivalents of pyruvate. Include mechanisms for each of these reactions.

2. What role does the conversion of an aldose to a ketose play in the net glycolytic reaction scheme?

3. Some organisms replenish the NAD^+ pool using alcoholic fermentation which yields ethanol and carbon dioxide. This is a 2 step process according to the following chemical scheme:

$$\text{Pyruvate} \rightleftharpoons \text{Acetaldehyde} + CO_2$$

$$\text{Acetaldehyde} + NADH + H^+ \rightleftharpoons \text{Acetaldehyde} + NAD^+$$

   a. How does this process "*complete*" glycolysis?
   b. What category of metabolic reactions do each of these fall into?
   c. Name the enzyme responsible for catalyzing each reaction (I suggest using KEGG for this). For each enzyme, name the enzyme class (e.g. hydrolase).
   d. Draw a mechanism for each of these reactions. Make sure to include any important cofactors.
   e. What role does the (+) charge on the TPP nitrogen play?

4. Glycolysis relies on 4 different phosphorylated variations of glycerate. What are these variations and what role do they play?

5. Determine how many equivalents of ATP are synthesized form one molecule of Glucose.

6. Determine how many equivalents of ATP are produced when four glucose units are removed from a glycogen polymer.

7. Phosphate transfer from PEP to ADP to yield ATP and enolpyruvate is not an exergonic process ($\Delta G^{o'} = 14.6$ kJ mol^{-1}). With this in mind, please propose a reason that PEP is a high energy phosphate compound that can transfer its phosphate to ADP in a net exergonic process under standard conditions.

8. The formation of oxonium ions are a staple in glycogen metabolism.
   a. What is the purpose of the oxoinum ion? Be specific – this was stressed in lecture.
   b. Show how the oxonium ion is used in the synthesis and degradation of glycogen.

9. Fat is much more prevalent and has a larger energy density (more ATP can be generated per volume) than glycogen. Why then is glycogen so important?

10. Glycogen Phosphorylase uses inorganic phosphate to generate glucose-1-phosphate (G1P) from glycogen
    a. How does G1P enter glycolysis?
    b. Why is it significant that this enzyme removes a glucose from the non-reducing end of glycogen?
11. Glycogen synthase uses UDP-glucose as a substrate for glycogen synthesis.
    a. What is the role of the UDP?
    b. Show how UDP-glucose is formed.
    c. What is glycogenin and why is it important in glycogen synthesis?

d. How is UTP regenerated and why is this significant when thinking about the energy landscape of this pathway?

12. Familiarize yourself with the JBC article below and answer the following questions:
    a. The *Thermoproteus tenax* genome contains two genes that code for a GAPDH. What is the difference in the chemical reaction catalyzed by these two proteins? What is the difference in cofactor dependence?
    b. The introduction to this article mentions two metabolic pathways that are able to convert glucose to pyruvate, the Embden-Meyerhof-Parnas and the Entner-Doudoroff pathways. Investigate these pathways.
        i. For the pathway that is different than what we've discussed, name and draw the structure of the 6 carbon intermediate that is cleaved into two 3 carbon units.
        ii. What are the two products and how are they related to glycolysis?
        iii. The enzyme that catalyzes this reaction is in the aldolase class of enzymes. Predict a mechanism.
    c. What does Figure 2 tell us about the enzyme of interest?
    d. How was enzyme activity monitored?
    e. Figure 5 has a lot of important information.
        i. What does this figure tell us about Glucose-1-phosphate and AMP – are they activators or inhibitors? Does this make sense based on the role of this enzyme?
        ii. The shape of the curve in the presence of $NADP^+$ is very different than the others. What does this tell us?
    f. Comment on the meaning of Hill coefficients determined in this paper.

ENZYMOLOGY:

NAD^+-dependent Glyceraldehyde-3-phosphate Dehydrogenase from *Thermoproteus tenax* : THE FIRST IDENTIFIED ARCHAEAL MEMBER OF THE ALDEHYDE DEHYDROGENASE SUPERFAMILY IS A GLYCOLYTIC ENZYME WITH UNUSUAL REGULATORY PROPERTIES

Nina A. Brunner, Henner Brinkmann, Bettina Siebers and Reinhard Hensel

J. Biol. Chem. 1998, 273:6149-6156.
doi: 10.1074/jbc.273.11.6149

THE JOURNAL OF BIOLOGICAL CHEMISTRY
Vol. 273, No. 11, Issue of March 13, pp. 6149–6156, 1998

Printed in U.S.A.

NAD^+-dependent Glyceraldehyde-3-phosphate Dehydrogenase from *Thermoproteus tenax*

THE FIRST IDENTIFIED ARCHAEAL MEMBER OF THE ALDEHYDE DEHYDROGENASE SUPERFAMILY IS A GLYCOLYTIC ENZYME WITH UNUSUAL REGULATORY PROPERTIES*

(Received for publication, November 3, 1997, and in revised form, January 2, 1998)

Nina A. Brunner, Henner Brinkmann‡, Bettina Siebers, and Reinhard Hensel§

From the Department of Microbiology, FB 9, Universität-GH Essen, Universitätsstrasse 5, 45117 Essen, Germany and the ‡Department of Cell Biology, Université Paris Sud, 91405 Orsay Cédex, France

The hyperthermophilic archaeum *Thermoproteus tenax* possesses two glyceraldehyde-3-phosphate dehydrogenases differing in cosubstrate specificity and phosphate dependence of the catalyzed reaction. NAD^+-dependent glyceraldehyde-3-phosphate dehydrogenase catalyzes the phosphate-independent irreversible oxidation of D-glyceraldehyde 3-phosphate to 3-phosphoglycerate. The coding gene was cloned, sequenced, and expressed in *Escherichia coli*. Sequence comparisons showed no similarity to phosphorylating glyceraldehyde-3-phosphate dehydrogenases but revealed a relationship to aldehyde dehydrogenases, with the highest similarity to the subgroup of nonphosphorylating glyceraldehyde-3-phosphate dehydrogenases.

The activity of the enzyme is affected by a series of metabolites. All effectors tested influence the affinity of the enzyme for its cosubstrate NAD^+. Whereas NADP(H), NADH, and ATP reduce the affinity for the cosubstrate, AMP, ADP, glucose 1-phosphate, and fructose 6-phosphate increase the affinity for NAD^+. Additionally, most of the effectors investigated induce cooperativity of NAD^+ binding.

The irreversible catabolic oxidation of glyceraldehyde 3-phosphate, the control of the enzyme by energy charge of the cell, and the regulation by intermediates of glycolysis and glucan degradation identify the NAD^+-dependent glyceraldehyde-3-phosphate dehydrogenase as an integral constituent of glycolysis in *T. tenax*. Its regulatory properties substitute for those lacking in the reversible nonregulated pyrophosphate-dependent phosphofructokinase in this variant of the Embden-Meyerhof-Parnas pathway.

With deeper insights into their physiology, the Archaea as the descendants of the third ancient lineage in the organismal evolution (1), have proved to be unexpectedly diverse. The central metabolic pathways of carbohydrate catabolism even exhibit a higher variability than found in Bacteria and Eucarya: in addition to modifications of the Entner-Doudoroff pathway (2, 3), several hitherto unknown variants of the classical Embden-Meyerhof-Parnas pathway have been described (4–6).

To address the diversification of the carbohydrate metabolism in Archaea and its regulation in response to growth conditions, we focused on *Thermoproteus tenax,* a hyperthermophilic crenarchaeote able to grow chemolithotrophically as well as chemoorganotrophically. Although a modified Entner-Doudoroff pathway is active in *T. tenax,* glucose is mainly degraded via a modified Embden-Meyerhof-Parnas pathway that is characterized by a reversible pyrophosphate-dependent phosphofructokinase (7). As an additional peculiarity, *T. tenax* possesses two pyridine nucleotide-dependent glyceraldehyde-3-phosphate dehydrogenases (GAPDHs)[1] that differ in their cosubstrate specificity (8). Whereas N-terminal sequence features revealed that the $NADP^+$-dependent GAPDH is a member of the common phosphorylating GAPDH of Archaea (E.C. 1.2.1.13), the structural affiliation of the NAD^+-dependent enzyme remained uncertain. An unusually high molecular mass (220 kDa) and the observation that the enzyme also exhibits activity without phosphate suggested a relationship to nonphosphorylating GAPDH (EC 1.2.1.9).

Nonphosphorylating GAPDH (GAPN) has been described as existing in diverse photosynthetic Eucarya such as plants, eucaryal microalgae, and protists (9–12), as well as in chemoorganotrophic bacteria (13). The enzymes characterized to date catalyze the irreversible oxidation of D-glyceraldehyde 3-phosphate (D-GAP) to 3-phosphoglycerate and show a high specificity for $NADP^+$ as cosubstrate. Due to the reaction catalyzed and the inhibition observed in the presence of intermediates of the oxidative pentose phosphate cycle and phosphohydroxypyruvate, an intermediate of the serine biosynthesis, it has been concluded that the enzymes fulfill mainly biosynthetic purposes by supplying NADPH for anabolic reactions or in serine biosynthesis (10, 13, 14). Sequence analyses of the genes encoding GAPN of pea and maize, as well as of the bacterium *Streptococcus mutans*, indicated that GAPN enzymes are not related to phosphorylating GAPDH at all, but belong to the superfamily of aldehyde dehydrogenases (ALDHs) (EC 1.2.1.3), which are characterized by varying degrees of substrate specificity (14, 15). Therefore, despite a similar catalytic mechanism, *i.e.* hydride transfer via a hemithioacetal intermediate, independent evolutionary origins of phosphorylating and nonphosphorylating GAPDH have been suggested. This is supported by the recently solved three-dimensional structure of two mammalian ALDHs (16, 17), in which differences regarding NAD^+ binding, topology of the catalytic domain, and subunit association clearly indicate a functionally convergent evolution of phosphorylating and nonphosphorylating GAPDH

* This work was supported by grants from the Deutsche Forschungsgemeinschaft and the Fonds der Chemischen Industrie. The costs of publication of this article were defrayed in part by the payment of page charges. This article must therefore be hereby marked "*advertisement*" in accordance with 18 U.S.C. Section 1734 solely to indicate this fact.

The nucleotide sequence(s) reported in this paper has been submitted to the GenBank™/EBI Data Bank with accession number(s) Y10625.

§ To whom correspondence should be addressed. Tel.: 0201-183-3442; Fax: 0201-183-2529; E-mail: bmb000@sp2.power.uni-essen.de.

[1] The abbreviations used are: GAPDH, glyceraldehyde-3-phosphate dehydrogenase (E.C. 1.2.1.12/E.C. 1.2.1.13); ALDH, aldehyde dehydrogenase; 3-PGA, 3-phosphoglycerate; GAP, glyceraldehyde 3-phosphate; GAPN, nonphosphorylating GAPDH; PCR, polymerase chain reaction.

enzymes. Here, we describe functional, structural, and regulatory properties of the NAD$^+$-dependent nonphosphorylating GAPDH of *T. tenax* and discuss them in terms of physiological and phylogenetic aspects.

EXPERIMENTAL PROCEDURES

Chemicals and Plasmids—D-GAP and DL-GAP were prepared from monobarium salts of the diethyl acetal (Sigma); all other chemicals (pro analysi grade) were from Fluka or Merck. Solutions of 1,3-bisphosphoglycerate were prepared as described previously (8). Cloning of PCR products and restriction fragments was performed using the plasmids pGEM T (Promega) and pBluescipt II KS+ (Stratagene), respectively. For heterologous expression, the vector pJF 118 EH was used (18).

Bacterial Strains and Growth Conditions—Mass cultures of *T. tenax* Kra 1 (DSM 2078) were grown as described previously (8). For cloning and expression experiments, the *Escherichia coli* strains XL1-Blue (Stratagene) and DH5α (Life Technologies) were grown under standard conditions (19).

Enzyme Assay—Enzymatic activity was measured as described previously (20). The standard assay for the oxidative reaction was performed at 70 °C containing 90 mM HEPES/KOH (pH 7.0 at 70 °C), 160 mM KCl, 20 mM NAD$^+$, and 4 mM DL-GAP. The reverse reaction was assayed in 90 mM HEPES/KOH (pH 8.0 at 45 °C), 160 mM KCl, 1 mM NADH, and 1–20 mM 3-PGA or 1,3-bisphosphoglycerate at 45 °C. Kinetic investigations were performed in 90 mM HEPES/KOH buffer (pH 7.0 at 70 °C) containing 160 mM KCl. Reactions were started by adding the substrate. The enzyme concentration ranged from 1 to 20 μg protein/ml.

Thermal stability tests, SDS-polyacrylamide gel electrophoresis, determination of protein concentration, and purification of the NAD$^+$-dependent GAPDH from *T. tenax* cells were performed as described previously (8).

Determination of K_D Values for Effectors—Apparent K_D values for effectors were calculated by following the decrease or increase of enzymatic activity with increasing concentrations of effector at 1 mM NAD$^+$ and 2 mM D-GAP.

CNBr Fragmentation and N-terminal Sequencing—Because the enzyme had been shown to be N-terminally blocked (8), the protein was cleaved with CNBr (21). The resulting peptides were separated by isoelectric focusing in the first dimension and by tricine-SDS-polyacrylamide gel electrophoresis in the second (22). Isoelectric focusing was performed using Immobiline Dry Strip gels (pH 4.0–7.0) in a Multiphor II isoelectric focusing system (Pharmacia) according to the manufacturer's instructions. Peptides and proteins were immobilized on Problott membranes (Applied Biosystems) by semidry electrotransfer (23). Sequencing was performed by automated Edman degradation in a gas phase sequencer 473A (Applied Biosystems). The following three peptides were isolated and their amino acid sequences were partially determined (pepide 2 overlaps with peptide 3 above position 30): peptide 1, RAGLLEGVIKEKGGVPVYPSTS; peptide 2, NAGKPKSAAVGEVKAAVDRLRLAELDLKKIGGDYIPGDWTYDTLETEGLVRREPPGV; peptide 3, PGAERLAVLRKAADIIERNLDVFAEVLVVNAGKPKSAAVGEEVKAAVDRLRLAELDLRKIGGDYI.

Cloning and Sequencing the Coding Gene—Genomic DNA was prepared as described by Weil *et al.* (24) modified according to Meakin *et al.* (25). The gene encoding NAD$^+$-dependent GAPDH was identified by hybridization with a homologous nucleotide probe generated by PCR amplification using the degenerate primers 5′GAYGTNTTYGCNGARGT3′ and 5′GTRTCRTANGTCCARTC3′, deduced from the hexapeptides DWTYDT and DVFAEV of the overlapping CNBr peptides 2 and 3. The PCR product comprising 156 nucleotides confirmed the protein sequence of the peptides except at position 29 of peptide 3, where the nucleotide sequence codes for methionine instead of valine, explaining the CNBr cleavage leading to peptide 2. For hybridization, the PCR product was labeled with digoxigenine according to the manufacturer's manual (Boehringer Mannheim). DNA was transferred to Biodyne B nylon membranes (Pall) by capillary blotting (26). Southern blots were hybridized at 68 °C in 5× SSC and stringently washed up to 68 °C in 0.1× SSC. A 3.0-kilobase *Spe*I fragment giving a strong hybridization signal was selected, cloned, and sequenced in an Automated Laser Fluorescent DNA Sequencer (Pharmacia) (27). The gene sequence was determined in both directions.

Expression of the Gene for NAD$^+$-dependent GAPDH from T. tenax in E. coli—For expression of the protein, the coding region was cloned into pJF 118 EH via two new restriction sites (*Eco*RI and *Sal*I) created by PCR mutagenesis with the primers 5′GTAGCCGTAGGAATATTATGAGGGCTGG3′ and 5′GGGAGTTGGTCGACTTGTGGCCAAGG3′. The sequence of the expression clone was confirmed by sequencing of both strands (27). Expression in *E. coli* DH5α cells was performed using standard procedures (19).

Purification of T. tenax NAD$^+$-dependent GAPDH from E. coli—10 g of *E. coli* cells were resuspended in 50 mM HEPES/KOH (pH 7.5) containing 7.5 mM dithiothreitol and passed three times through a French press cell at 150 megapascals. After centrifugation (20,000 × *g* for 20 min) the solution was heat-precipitated (90 °C for 30 min) and centrifuged again. Homogeneous enzyme preparations were achieved by chromatography on hydroxylapatite High Resolution (Fluka) and blue Sepharose CL6B (Pharmacia) as described previously (8). The N terminus was not blocked, in contrast to the protein isolated from *T. tenax* cells. Edman degradation confirmed the N-terminal sequence of the recombinant protein (MRAGL, see above).

Phylogenetic Analysis—For sequence analysis and computer alignments, the programs GENMON, version 4.4 (GBF Braunschweig), and CLUSTAL W (28) were used. Homology searches were performed with BLASTP and BLASTX via MEDLINE. The source of sequence information was GenBank (update, June 1997). Phylogenetic trees were calculated with the PHYLIP program package, version 3.5c (29), and reliability of branches was estimated by bootstrap analyses. The PAUP program, version 3.1, was used for maximum parsimony analysis of protein sequences, including bootstrap replicates.

RESULTS

Nucleotide Sequence of the Gene Coding for NAD$^+$-dependent GAPDH from T. tenax—The sequence analysis revealed a single open reading frame comprising 1503 base pairs (Fig. 1, positions 130–1632) corresponding to a polypeptide of 501 amino acid residues with a calculated molecular mass of 55 kDa. The deduced amino acid sequence corresponds with the partial amino acid sequences of the three CNBr fragments prepared from the protein and a tryptic peptide published earlier (8), thus identifying the open reading frame as the coding gene for the NAD$^+$-dependent GAPDH. The translation start could not be determined by Edman degradation, presumably due to N-terminal modification. Translation is probably initiated at the AUG codon of positions 130–132, where the encoded methionyl residue represents the N-terminal cleavage site of CNBr peptide 1, because in the upstream region no potential start codon was found up to the next in-frame stop codon at position 106–108. In front of the coding region, a sequence resembling the boxA element of archaeal promoters was identified, suggesting functional importance as transcriptional signal. A putative ribosome binding site is located at positions 119–124, matching the complementary 3′-end of the 16S rRNA of *T. tenax* (30).

Deduced Amino Acid Sequence of the NAD$^+$-dependent GAPDH: Comparison with Homologous Proteins—The NAD$^+$-dependent GAPDH shows significant sequence similarity with aldehyde dehydrogenases of various sources but not with phosphorylating GAPDH from Bacteria, Eucarya, or Archaea. The close relationship of the *T. tenax* enzyme to ALDH is reflected by accordance in active site residues assigned on the basis of the recently resolved three-dimensional structure of rat liver ALDH3 (Fig. 2) and bovine ALDH2 (16, 17). The comparison shows that in addition to the catalytically essential Glu-209 (263) and Cys-243 (297), all residues involved in NAD$^+$ binding are strictly conserved in the *T. tenax* sequence: Asn-114 (168), Thr-186 (242), Gly-187 (243), Leu-210 (264), Gly-211 (265), and Phe-335 (397) (numbering according to the ALDH3 sequence; numbers in parentheses refer to *T. tenax*) (see Fig. 2). The highest overall similarity was detected to GAP-specific ALDH from pea and maize (31.1 and 31.4% amino acid identity, respectively) and from the bacterium *S. mutans* (33.5% identity; Fig. 2), characterized as GAPN.

Phylogenetic Analyses—Phylogenetic analyses using parsimony and distance matrix (neighbor-joining) methods were performed with various representatives of the ALDH superfamily (Fig. 3), including the predicted protein sequences of

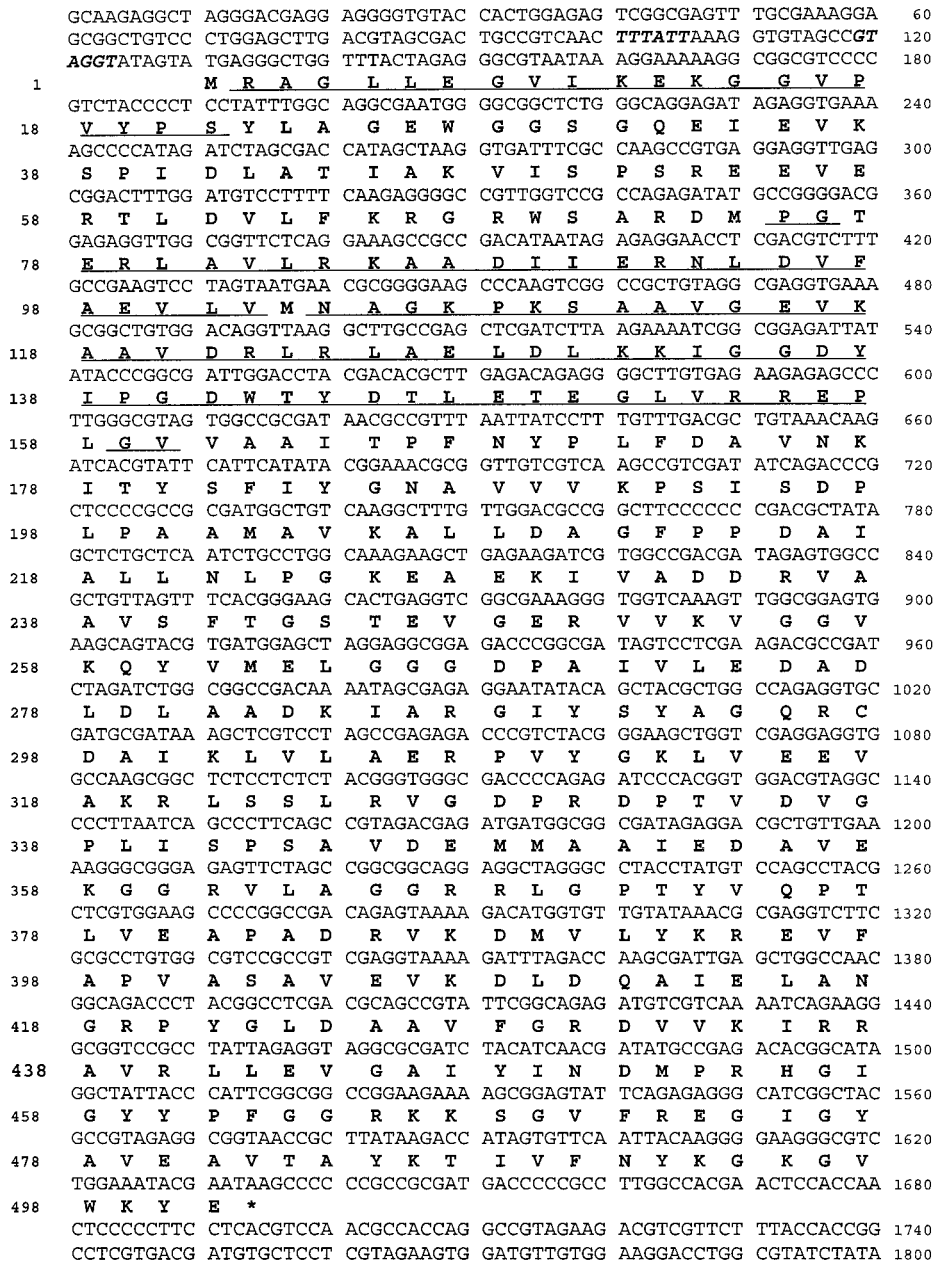

FIG. 1. **Nucleotide sequence of the *gapN* gene from *T. tenax* and its flanking regions.** The deduced amino acid sequence is shown *below* in the one-letter code; residues confirmed by Edman degradation of CNBr peptides are *underlined*. The nucleotide sequences of the putative promoter box A element and the ribosome binding site are shown in *boldface italics* (positions 101–106 and 119–124, respectively).

genes from the genomes of *Methanococcus jannaschii* (31), *Synechocystis* sp. (32), and *Rhizobium meliloti* (33). The analyses resulted in a complex tree topology similar to that found by Habenicht *et al.* (14), which is characterized by several poorly resolved lineages comprising enzymes of different substrate specificities (Fig. 3). The NAD$^+$-GAPDH of *T. tenax* is affiliated with the GAPN from plants and *S. mutans*. Although this branch is not robustly supported by bootstrap analysis, the affiliation of *T. tenax* GAPDH with the GAPN-subtree is assured by several unique sequence signatures (Fig. 2) (GEW (26–28), EEV (55–57), PFNYP (106–170), IVLEDADL (271–278), and GQRC (294–297) (numbers in parentheses are the positions of the *T. tenax* sequence).

Expression of the Gene Encoding NAD$^+$-dependent GAPDH in E. coli and Comparison of the Recombinant Protein with the Enzyme Isolated from T. tenax Cells—For functional and structural studies, the gene encoding NAD$^+$-dependent GAPDH (*gapN*) was expressed in *E. coli*. As calculated from the specific activity of the purified enzyme (Table I and Fig. 4), the expression efficiency in *E. coli* was relatively low (1% of the total soluble protein was recombinant GAPDH). Comparisons between the GAPDH isolated from *T. tenax* and the recombinant enzyme revealed no differences with respect to molecular mass and enzymic properties, such as kinetic parameters of cosubstrate saturation in the presence and absence of the effector AMP (Table I).

With respect to thermal stability, the recombinant enzyme differed from the enzyme isolated from *T. tenax* cells. Although both enzymes showed the same initial inactivation rates at 100 °C (pseudo-first order kinetics: $t_{1/2}$ = 25 min up to 30 min of incubation), the inactivation rates differed with preceding incubation time: the activity of the enzyme isolated from *T. tenax* cells decreased less dramatically, resulting in a residual activity of 30% after 100 min of incubation compared with 10% for the recombinant enzyme. Possibly, the modification responsible for the N-terminal block of the protein from *T. tenax* influences its thermal stability.

Reaction Catalyzed by the Enzyme—Contrary to previous results (8), enzyme preparations from *T. tenax* cells did not show activity in the reverse reaction, neither with 1,3-bisphos-

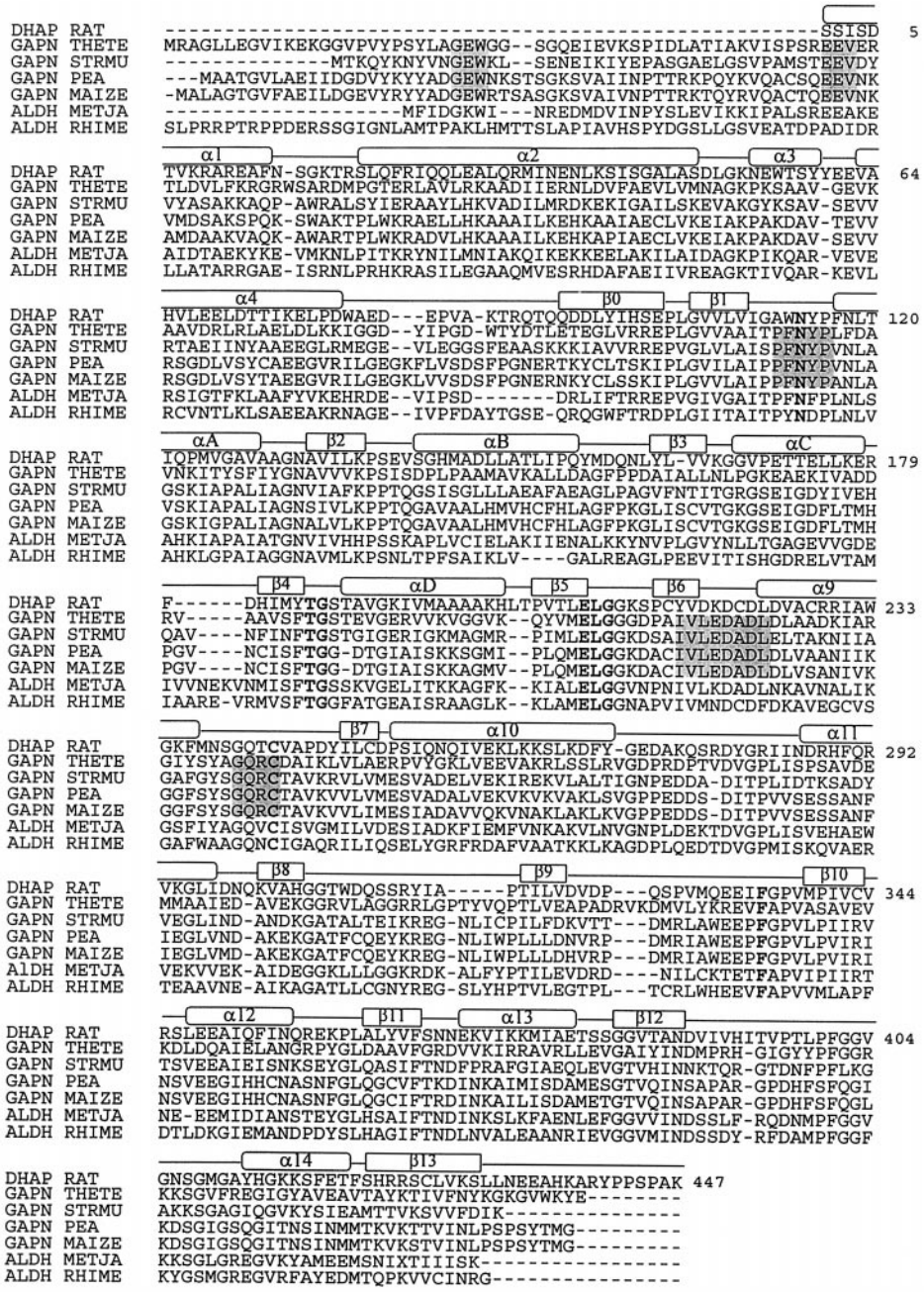

FIG. 2. **Amino acid sequence alignment of the NAD$^+$-dependent GAPDH from *T. tenax* with various ALDHs.** Gaps introduced for optimal alignment are indicated by *hyphens*. Conserved functional residues are in *boldface* and unique sequence signatures of nonphosphorylating GAPDHs are *shaded*. Amino acid positions and secondary structure elements (α, α-helix; β, β-strand) of the ALDH3 from rat liver (17) are given *above* the sequences. Origin of sequences: *DHAP RAT*, ALDH3 of rat liver (17); *GAPN THETE*, nonphosphorylating GAPDH of *T. tenax* (this study); *GAPN STRMU*, nonphosphorylating GAPDH of *S. mutans* (15); *GAPN PEA*, nonphosphorylating GAPDH of *Pisum sativum* (14); *GAPN MAIZE*, nonphosphorylating GAPDH of *Zea mays* (14); *ALDH METJA*, unspecified ALDH from *M. jannaschii* (31); *ALDH RHIME*, unspecified ALDH from *R. meliloti* (33).

phoglycerate nor with 3-PGA as substrate (range of 1,3-bisphosphoglycerate or 3-PGA, 0.5–10 mM), strongly suggesting that the enzyme works exclusively in the oxidative direction like all other ALDHs known at present. The irreversibility of the reaction could also be confirmed with the recombinant enzyme. Possibly, impurities in the previous enzyme preparations mimicked a reversible reaction. For analyzing further enzymic properties of the enzyme, such as substrate or cosubstrate specificity, and the effect of various metabolites on the enzyme activity, we exclusively used the functionally equivalent but more convenient recombinant enzyme.

The enzyme proved to be specific for D-GAP. L-GAP acts as strong competitive inhibitor with respect to D-GAP (K_i = 130 μM). As a consequence, saturation kinetics with a racemic mixture of D-isomer and L-isomer revealed a 50% lower V_{max}. The saturation with D-GAP followed classical Michaelis-Menten kinetics, showing half-maximal saturation at 50 μM. A definite K_m for the free aldehyde, the presumed substrate of the enzyme, cannot be given because the portion of the free aldehyde in aqueous solution could not be determined at 70 °C. None of the following aldehydes and alcohols (concentration range, 0.5–20 mM) tested for their ability to act as substrates (assay without substrate) and to compete for the active site (assay in the presences of half-saturating substrate concentration) were accepted by the enzyme: formaldehyde, acetaldehyde, propionaldehyde, *n*-valeraldehyde, butyraldehyde, benzaldehyde, hexanal, glyceraldehyde, glycolic aldehyde, succinic semialdehyde, and betaine aldehyde. The enzyme uses exclusively NAD$^+$ as a cosubstrate (apparent K_m of NAD = 3.0 mM). NADP$^+$ cannot replace NAD$^+$ but acts as strong inhibitor (see below).

Effectors of the NAD$^+$-dependent GAPDH—Several metabolites, including NADP$^+$, NADPH, NADH, and the adenine nucleotides ATP, ADP, and AMP, were tested under nonsaturating substrate and cosubstrate concentrations (0.2 mM D-GAP; 1 mM NAD$^+$) as possible effectors for the enzyme. Virtually no effects were observed with dihydroxyacetone phosphate, phosphoenol pyruvate, coenzyme A, erythrose 4-phosphate, xylose

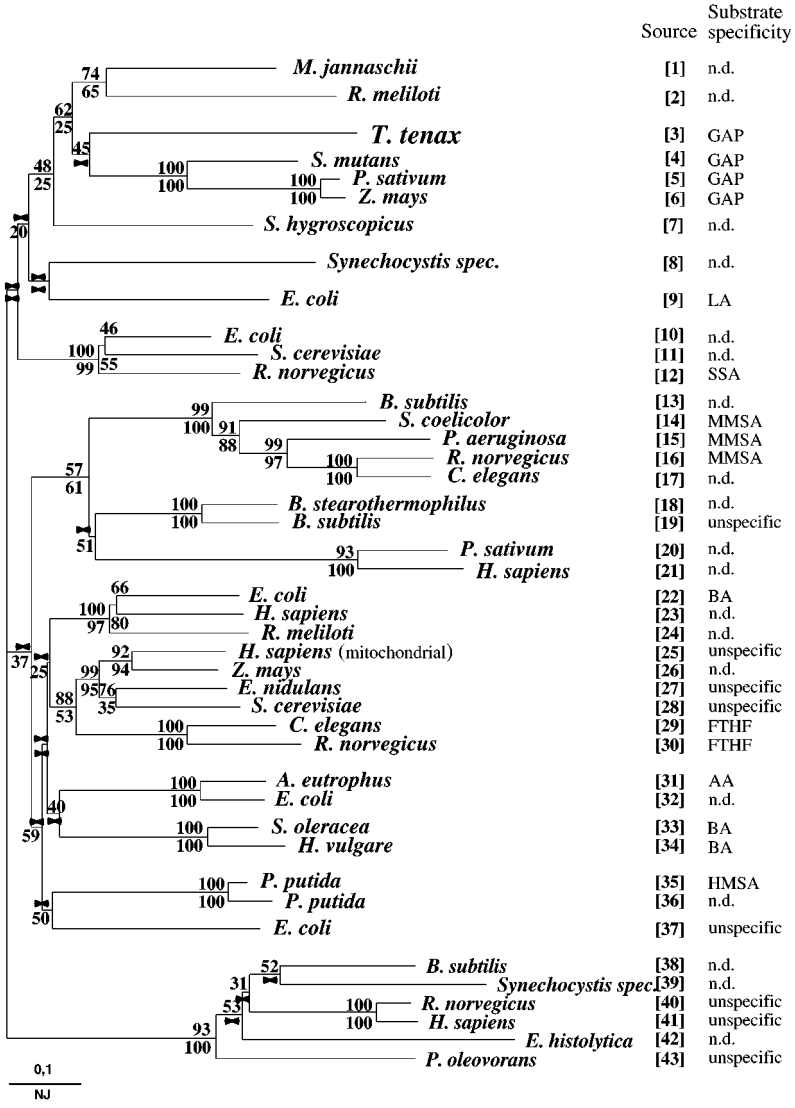

FIG. 3. **Phylogenetic tree of ALDHs including 42 representatives of the ALDH superfamily (available in GenBank) and the sequence of NAD$^+$-dependent GAPDH from *T. tenax*.** The tree was constructed by the Neighbor Joining algorithm (48) based on distances calculated from the protein alignment using the Kimura correction (49). The *scale bar* corresponds to 0.1 nonsynonymous substitution per site; *numbers* at nodes indicate bootstrap values (Neighbor Joining/Parsimony) for 100 replicates. Enzymes are abbreviated as follows: (1) *M. jannaschii*, gi 1592060; (2) *R. meliloti*, gi 1486426; (3) *T. tenax*, sp Y10625; (4) *S. mutans*, gi 642667; (5) *P. sativum*, pir S43832; (6) *Z. mays*, pir S43833; (7) *Streptomyces hygroscopicus*, sp D37877; (8) *Synechocystis* sp., gi 1001464; (9) *E. coli*, sp P25553; (10) *E. coli*, sp P25526; (11) *Saccharomyces cerevisiae*, sp P38067; (12) *Rattus norvegicus*, gi 556395; (13) *Bacillus subtilis*, sp P42412; (14) *Streptomyces coelicolor*, gi 1041092; (15) *Pseudomonas aeruginosa*, sp P28810; (16) *R. norvegicus*, sp Q02253; (17) *Caenorhabditis elegans*, gi 790381; (18) *Bacillus stearothermophilus*, sp P42329; (19) *Bacillus subtilis*, sp P42236; (20) *P. sativum*, sp P25795; (21) *Homo sapiens*, sp P49419; (22) *E. coli*, sp P17445; (23) *H. sapiens* sp P49189; (24) *R. meliloti*, gi 1086574; (25) *H. sapiens*, sp P05091; (26) *Z. mays*, gi 1421730; (27) *Aspergillus nidulans*, sp P08157; (28) *S. cerevisiae*, sp P32872; (29) *C. elegans*, gi 11677954; (30) *R. norvegicus*, sp P28037; (31) *Alcaligenes eutrophus*, sp P46368; (32) *E. coli*, pir S47809; (33) *Spinacea oleracea*, sp P17202; (34) *Hordeum vulgare*, gi 927643; (35) *Pseudomonas putida*, sp P23105; (36) *P. putida*, sp P19059; (37) *E. coli*, sp P23883; (38) *Bacillus subtilis*, sp P39616; (39) *Synechocystis* sp., gi 1001727; (40) *R. norvegicus*, sp P11883; (41) *H. sapiens*, sp P30838; (42) *Entamoeba histolytica*, sp P30840; (43) *Pseudomonas oleovorans*, sp P12693. Substrate specificities are abbreviated as follows: *LA*, lactaldehyde; *SSA*, succinate semialdehyde; *MMSA*, methylmalonate semialdehyde; *BA*, betaine aldehyde; *FTHF*, 10-formyltetrahydrofolate; *HMSA*, 2-hydroxymuconic semialdehyde.

5-phosphate, fructose 1,6-phosphate, or sedoheptulose 7-phosphate, whereas NADP$^+$, NADPH, NADH, and ATP acted as potent inhibitors (apparent K_D = 0.3–3000 μM, as calculated from their concentration-dependent inhibition) (Table II). ADP, AMP, glucose 1-phosphate, glucose 6-phosphate, fructose 1-phosphate, fructose 6-phosphate, and ribose 5-phosphate acted as activators (apparent K_D = 1.0–2500 μM, as calculated from their concentration-dependent activation) (Table II). NADPH and glucose 1-phosphate proved to be the most affine effectors, exhibiting apparent K_D values of 0.3 μM and 1.0 μM, respectively, under the conditions applied. In the presence of both NADPH and glucose 1-phosphate at equivalent concentrations (10 μM), the effect of the activator predominated, resulting in a 2-fold higher activity as compared with the control without effector. The compensating effect of glucose 1-phosphate on the inhibitory action of NADPH was also reflected by an approximately 200-fold lowering of the apparent K_D of NADPH in the presence of 10 μM glucose 1-phosphate (apparent K_D of NADPH = 56 μM; data not shown). Mg^{2+} ions did not affect the enzymic properties, either alone or in combination with adenine nucleotides.

The effects of NADP$^+$, NADH, ATP, ADP, AMP, and glucose 1-phosphate on the activity of the enzyme were studied in more detail by investigating the influence on NAD$^+$ and D-GAP binding at saturating concentrations of the nonvaried substrate. All ligands affect exclusively the affinity of the enzyme for NAD$^+$.

TABLE I
Enzymic, macromolecular, and stability properties of the NAD⁺-dependent GAPDH from T. tenax: comparison with the recombinant enzyme

	NAD⁺-dependent GAPDH of *T. tenax*	
	Isolated from *T. tenax*	Isolated from *E. coli*
NAD⁺ saturation[a]		
Without AMP		
V_{max} (units/mg)	36.5	38.0
K_m (mM)	3.3	3.1
In the presence of AMP		
V_{max} (units/mg)	37.0	37.5
K_m (mM)	1.4	1.5
Arsenate saturation[b]		
V_{max} (units/mg)	37.0	39.0
Apparent K_D (mM)	75.0	75.0
Thermal stability[c]		
Residual activity (%) after 100 min at 100 °C	30	10
Molecular mass		
Subunit (kDa)	55,000	55,000
Native (kDa)	220,000	220,000

[a] Assay conditions: 90 mM HEPES (pH 7.0), 160 mM KCl, 4 mM DL-GAP, +/− 860 μM AMP.
[b] Assay conditions: 90 mM HEPES (pH 7.0), 4 mM DL-GAP, 10 mM NAD⁺.
[c] Assay conditions: 10 mM HEPES (pH 7.0), 7.5 mM DTT. Protein concentration, 30 μg/ml.

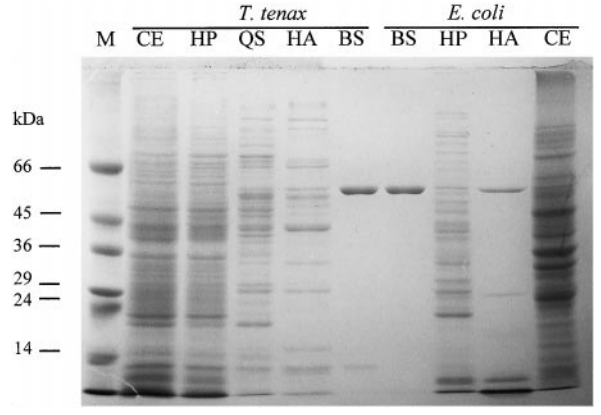

FIG. 4. **Electropherogram of SDS-polyacrylamide gel electrophoresis documenting the purification of the NAD⁺-dependent GAPDH from *T. tenax* and from *E. coli* cells.** *M*, molecular mass standard; *CE*, crude extract; *HP*, fraction after heat precipitation; *QS*, fraction after separation on Q-Sepharose; *HA*, fraction after chromatography on hydroxylapatite; *BS*, fractions after chromatography on blue Sepharose.

Additionally, most of the effectors induce positive cooperativity of cosubstrate binding (Table III and Fig. 5), with maximal Hill coefficients of 1.9 as exhibited by NADH.

DISCUSSION

NAD⁺-dependent GAPDH of T. tenax, a Member of the ALDH Superfamily—Reaction type and sequence features classify the NAD⁺-dependent GAPDH of *T. tenax* as ALDH. As such, the enzyme represents the first biochemically characterized archaeal member of this highly diverse protein family, which comprises a variety of enzymes differing in their enzymic properties, including substrate and cosubstrate specificity and mode of catalysis (14, 34). Regarding the high substrate specificity for D-GAP and the phosphate independence of the catalyzed oxidation of the aldehyde to the corresponding acid, 3-PGA, the *T. tenax* enzyme resembles most the ALDH subgroup of NADP⁺-specific GAPN. Differences from presently known GAPN exist with respect to cosubstrate specificity and regulatory properties.

TABLE II
Apparent K_D values of various metabolites as deduced from their activating or inhibitory effects

Measurements were performed at nonsaturating concentrations of NAD⁺ (1 mM NAD⁺) and at saturating concentrations of D-GAP (2 mM).

Metabolite tested	Apparent K_D
	μM
Inhibitors	
NADPH	0.3
NADP⁺	1.0
NADH	30
ATP	3000
Activators	
Glucose 1-phosphate	1.0
AMP	140
Fructose 6-phosphate	200
ADP	250
Fructose 1-phosphate	1700
Ribose 5-phosphate	2500

TABLE III
Effect of various metabolites on cosubstrate binding to the NAD⁺-dependent GAPDH of T. tenax

Metabolite tested	Apparent K_m of NAD or $S_{0.5}$ of NAD	Hill coefficient
	mM	
None	3.1	1.0
0.05 mM NADP⁺	4.5	1.6
0.10 mM glucose 1-phosphate	0.4	1.1
0.43 mM NADH	8.0	1.9
0.86 mM AMP	1.3	1.5
0.86 mM ADP	1.7	1.2
17.0 mM ATP	30	1.4

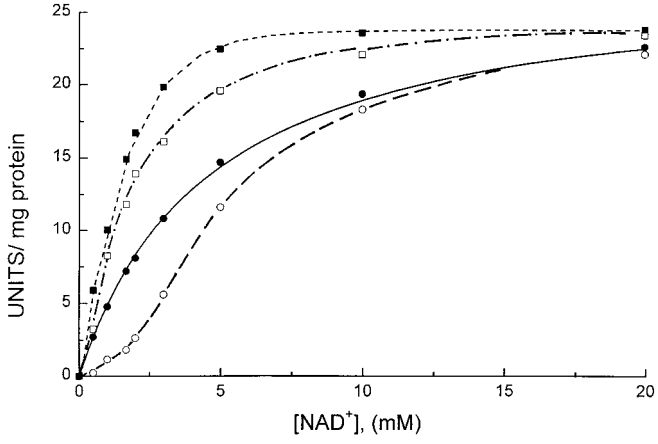

FIG. 5. **Cosubstrate saturation of NAD⁺-dependent GAPDH of *T. tenax* in the presence of various effectors.** Assay conditions: 90 mM HEPES (pH 7.0), 160 mM KCl, 4 mM DL-GAP. ●, control; ○, 50 μM NADP⁺; ■, 100 μM glucose 1-phosphate; □, 1 mM AMP.

Phylogeny—Despite rather low bootstrap support (45%, neighbor joining), the affiliation of the *T. tenax* enzyme with the GAPN lineage is revealed by unique sequence signatures (Fig. 2). Two of these sequences (GQRC and PFNYP) could be assigned to the active site region on the basis of crystallographic studies of mammalian ALDH (16, 17), emphasizing their importance for evolutionary affinity. The first fragment harbors the catalytically essential cysteinyl residue (corresponding to Cys-234 in the rat liver ALDH3), and the second contains a functionally important asparaginyl residue (corresponding to Asn-114 in the rat liver ALDH3) interacting with the nicotinamide ring of the cosubstrate. The functional importance of a third signature sequence (IVLEDADL) is still speculative. On the basis of the three-dimensional structure of the mammalian ALDH, it is part of the loop region between β_1 and

α_A helix of a second α/β dinucleotide binding fold constituting most of the catalytic domain. Because this loop interacts commonly with the phosphate moiety of nucleotides in nucleotide-binding proteins, it is conceivable that this region assumed the function of effector binding in GAPN.

Because the monophyletic GAPN subtree comprises members of all three domains (it is presumed that the relationship between GAPN enzymes is not confounded by lateral gene transfer events), it appears that the GAPN lineage originated prior to the divergence of the domains.

As shown in Fig. 3, the root of the GAPN subtree implied by the deeper branching lineages, leading to the uncharacterized ALDHs of *R. meliloti, M. jannaschii*, or *S. hygroscopicus*, indicates a closer affinity between eucaryal and bacterial GAPN under the exclusion of the archaeal homolog of *T. tenax*. As such, the branching order does not coincide with the "conventional" topology of rooted universal trees constructed with elongation factors, aminoacyl-tRNA synthetases, and ATPases (36–38), showing the archaeal and eucaryal homologs as sister groups and the bacterial counterparts as earliest diverging line. Thus, with the presently available GAPN homologues a universal-tree topology could be verified, which may reflect the bacterial inheritance of the eucaryal genome. This topology is also supported by the preferred similarity between the bacterial and eucaryal homologs of several metabolic enzymes, such as phosphorylating GAPDH, 3-phosphoglycerate kinase, and triosephosphate isomerase (39–43).

The other, apparently more deeply rooting branches in Fig. 3 bear both bacterial and eucaryal sequences. They may witness an intense gene diversification already in the progenote, as recently suggested (14). Alternatively, because no archaeal members within these lineages could be identified yet, they may reflect bacterial ALDH radiation, whereby the interlacing of bacterial and eucaryal ALDHs could be due to the bacterial origin of eucaryal ALDH genes.

Allosteric Regulation—One of the most striking features of the *T. tenax* enzyme is its regulation by metabolites, which is not only more pronounced than that of all GAPNs but also of all ALDHs characterized to date. As a main difference from eucaryal and bacterial GAPN, the NAD$^+$-dependent GAPDH of *T. tenax* is not only inhibited but also activated by a series of metabolites. Until now, stimulating effects could only be described for the *S. mutans* GAPN (13) with cations such as NH_4^+ and K^+. But this activation is rather due to decreasing substrate inhibition and probably not of physiological relevance. Generally, little is known about the regulation capacity of other ALDHs with broad or narrow substrate specificity. Activation by Mg^{2+} ions has been reported for the mitochondrial ALDH from horse liver or rat testis (44, 45). Furthermore stimulation of the esterolytic activity of ALDH by NAD$^+$ or NADH has been described with a more pronounced effect of pyridine nucleotides (and also coenzyme A) observed in the case of methylmalonate semialdehyde dehydrogenase (34). Still, it is an open question whether the hydrolytic activity of ALDH is of physiological importance.

At present, our structural and functional information is too scarce to deduce a consistent model for the effector-induced substrate or cosubstrate binding of the *T. tenax* enzyme. At least, Hill coefficients of (maximally) 2, determined for the NAD$^+$ binding of the *T. tenax* enzyme in the presence of effectors, are consistent with the subunit arrangement of the mammalian ALDH expecting cooperativity between the two closely neighbored cosubstrate binding sites.

No information is available about the binding site(s) of the different effectors or about the conformational changes caused by them. On the basis of the known three-dimensional structure of ALDH, one may speculate that effector binding of the nonphosphorylating GAPDH occurs at the catalytic domain. In the ALDH structure model, the subunit contains two α/β dinucleotide binding folds; the first (functional) fold is located in the NAD$^+$ binding domain, and the second (obviously functionless) fold is found in the catalytic domain. The suggestion that in GAPN, including the *T. tenax* enzyme, the second dinucleotide binding unit may be involved in effector binding is based mainly on the finding that in these enzymes a specific sequence conservation could be observed concerning a region that corresponds to the loop region connecting β_1 and α_A of that second dinucleotide binding unit. The close vicinity of the presumed effector site to the NAD$^+$ binding pocket and to the dimer-intersubunit contacts would explain the effector-mediated influence on both NAD$^+$ binding affinity and cooperativity.

Physiological Role—From the pattern of regulation, conclusions about the physiological role of the *T. tenax* enzyme can be drawn. The observation that the activity of the enzyme is controlled mainly by the energy charge of the cell and by intermediates of glucan polymer degradation (glucose 1-phosphate) and glycolysis (fructose 6-phosphate) accounts for a catabolic role of the enzyme, which thus differs from eucaryal or bacterial GAPN with obvious anabolic function (10, 13).

T. tenax possesses two catabolic pathways for glucose, the modified (nonphosphorylative) Entner-Doudoroff pathway and a variant of the Embden-Meyerhof-Parnas pathway representing the dominant catabolic route in cells grown on glucose (6, 7, 46). From its reaction type and regulation pattern, the NAD$^+$-dependent nonphosphorylating GAPDH fits into the catabolic reaction sequence of the Embden-Meyerhof-Parnas pathway of this organism.

Previous suggestions based on the strong inhibition of the enzyme by NADP$^+$ suggested an *in vivo* activity only at late stationary phase, when the intracellular concentration of the inhibitor is sufficiently low. But in fact, the enzyme also seems to be active under normal growth conditions because the enzyme exhibits activity despite strong inhibition by NADP$^+$ and NADPH as soon as activators are simultaneously present. Glucose 1-phosphate proved to be the most potent activator. It represents the first intermediate in the degradation of glycogen, a reserve polymer that has been previously documented in *T. tenax* (47). As reported here, 10 μM glucose 1-phosphate is sufficient to reduce the affinity of the enzyme for the strongest inhibitor NADPH by a factor of 200. From the *in vitro* experiments, we must therefore assume a tight *in vivo* regulation of the enzyme, allowing activity only at a low ATP/ADP+AMP ratio and/or in the presence of activating intermediates, such as glucose 1-phosphate and fructose 6-phosphate. Whether the activation by fructose 1-phosphate and ribose 5-phosphate is of physiological relevance, exhibiting a significantly lower affinity for the enzyme, remains to be established.

With its regulatory properties, NAD$^+$-dependent GAPDH fulfills the control function commonly executed by the enzyme couple ATP-dependent phosphofructokinase/fructose-1,6-bisphosphatase in glycolysis, which is substituted by the reversible nonregulated PP_i-phosphofructokinase in *T. tenax*. Furthermore, the irreversible reaction catalyzed by the NAD$^+$-dependent GAPDH of *T. tenax* drives the carbon flux into the catabolic direction of the pathway. Thus, the enzyme seems to compensate not only the lacking regulatory properties of the reversible PP_i-phosphofructokinase but also its driving force for the catabolic reaction. This ability is gained at the expense of 2 mol of ATP/mol of glucose, which would be additionally generated using a phosphorylating but reversible GAPDH. Thus, the principal physiological function of the NAD$^+$-dependent GAPDH should reside in an increase of the catabolic rate and the recovery of compounds such as 3-PGA, phosphoenolpyruvate, or

pyruvate, allowing a more rapid availability of ATP and/or precursors for biosynthetic purposes. In terms of a high glycolytic energy yield, however, the use of the phosphorylating NADP$^+$-dependent GAPDH should be more effective. Therefore, the possibility cannot be excluded that under conditions of high energy demand this enzyme is active in catabolism as well, despite a higher V_{max} for the reductive reaction, suggesting an anabolic role (8).

Acknowledgments—We thank Dr. W. F. Martin (TU Braunschweig) and Dr. R. Sterner (Biocenter Basel, Switzerland) for critically reading the manuscript and Prof. R. Cerff (TU Braunschweig) for valuable discussions. We are indebted to M. Schubert (Technical University, Braunschweig) for advice on methodical questions.

REFERENCES

1. Woese, C. R., and Fox, G. E. (1977) *Proc. Natl. Acad. Sci. U. S. A.* **74,** 5088–5090
2. Danson, M. J., Hough, D. W. and Lunt, G. G. (1992) *The Archaebacteria*, pp. 7–13, Portland Press, London
3. Schönheit, P., and Schäfer, T. (1995) *World J. Microbiol. Biotechnol.* **11,** 26–57
4. Altekar, W., and Rangaswamy, V. (1992) *Arch. Microbiol.* **158,** 356–363
5. Kengen, S. W. M., de Bok, F. A. M., van Loo, N.-D., Dijkema, C., Stams, A. J. M., and de Vos, W. M. (1994) *J. Biol. Chem.* **269,** 17537–17541
6. Selig, M., Xavier, K. B., Santos, H., and Schönheit, P. (1997) *Arch. Microbiol.* **167,** 217–232
7. Siebers, B., and Hensel, R. (1993) *FEMS Microbiol. Lett.* **111,** 1–8
8. Hensel, R., Laumann, S., Lang, J., Heumann, H., and Lottspeich, F. (1987) *Eur. J. Biochem.* **170,** 325–333
9. Arnon, D. I., Rosenberg, L. L., and Whatley, R. F. (1954) *Nature* **173,** 1132–1134
10. Kelly, G. J., and Gibbs, M. (1973) *Plant Physiol.* **52,** 111–118
11. Iglesias, A. A., and Losada, M. (1988) *Arch. Biochem. Biophys.* **260,** 830–840
12. Mateos, M. I., and Serrano, A. (1992) *Plant Sci.* **84,** 163–170
13. Crow, V. L., and Wittenberger, C. L. (1979) *J. Biol. Chem.* **254,** 1134–1142
14. Habenicht, A., Hellmann, U., and Cerff, R. (1994) *Mol. Biol.* **237,** 165–171
15. Boyd, D. A., Cvitkovitch, D. G., and Hamilton, I. R. (1995) *J. Bacteriol.* **177,** 2622–2627
16. Liu, Z.-J., Sun, Y.-J., Rose, J., Chung, Y.-J., Hsiao, C.-D., Chang, W.-R., Kuo, I., Perozich, J., Lindahl, R., Hempel, J., and Wang, B.-C. (1997) *Nat. Struct. Biol.* **4,** 317–326
17. Steinmetz, C. G., Xie, P., Weiner, H., and Hurley, T. D. (1997) *Structure* **5,** 701–711
18. Fürste, J. P., Pansegrau, W., Frank, R., Blöcker, H., Scholz, P., Bagdasarian, M., and Lanka, E. (1986) *Gene* **48,** 119–131
19. Sambrook, J., Fritsch, E. F., and Maniatis, T. (1989) *Molecular Cloning: A Laboratory Manual* 2nd Ed., Cold Spring Harbor Laboratory, Cold Spring Harbor, NY
20. Fabry, S., and Hensel, R. (1987) *Eur. J. Biochem.* **165,** 147–155
21. Fontana, A., and Gross, E. (1986) *Practical Protein Chemistry: A Handbook*, pp. 83–83, Wiley & Sons Ltd., Chichester, United Kingdom
22. Schägger, H., and von Jagow, G. (1987) *Anal. Biochem.* **166,** 368–379
23. Jungblut, P., Eckerskorn, C., Lottspeich, F., and Klose, J. (1990) *Electrophoresis* **11,** 581–588
24. Weil, C. F., Cram, D. S., Sherf, B. A., and Reeve, J. N. (1988) *J. Bacteriol.* **170,** 4718–4726
25. Meakin, S. A., Nash, J., Murray, W. D., Kennedy, K. J., and Sprott, G. D. (1991) *J. Microbiol. Methods* **14,** 119–126
26. Chomczynski, P. (1992) *Anal. Biochem.* **201,** 134–139
27. Wiemann, S., Rupp, T., Zimmermann, J., Voss, H., Schwager, C., and Ansorge, W. (1995) *BioTechniques* **18,** 688–697
28. Higgins, D. G. (1994) *Methods Mol. Biol.* **25,** 307–318
29. Felsenstein, J. (1996) *Methods Enzymol.* **266,** 418–427
30. Leinfelder, W., Jarsch, M., and Böck, A. (1985) *Syst. Appl. Microbiol.* **6,** 164–170
31. Bult, C. J., White, O., Olsen, G. J., Zhou, L., Fleischmann, R. D., Sutton G. G., Blake, J. A., FitzGerald, L. M., Clayton, R. A., Gocayne, J. D., Kerlavage, A. R., Dougherty, B. A., Tomb, J. F., Adams, M. D., Reich, C. I., Overbeek, R., Kirkness, E. F., Weinstock, K. G., Merrick, J. M., Glodek, A., Scott, J. L., Geoghagen, N. S. M., and Venter, J. C. (1996) *Science* **273,** 1058–1073
32. Kaneko, T., Tanaka, A., Sato, S., Kotani, H., Sazuka, T., Miy sugiura, M., and Tabata, S. (1995) *DNA Res.* **2,** 153–166
33. Freiberg, C., Perret, X., Broughton, W., and Rosenthal, A. (1996) *Genome Res.* **6,** 590–600
34. Popov, K. M., Kedishvili, N. Y., and Harris, R. A. (1992) *Biochem. Biophys. Acta* **1119,** 69–73
35. Hidaka, T., Hidaka, M., Kuzuyama, T., and Seto, H. (1995) *Gene* **158,** 149–150
36. Gogarten, J.-P., Kibak, H., Dittrich, P., Taiz, L., Bowman, E.-J., Bowman, B. J., Manolson, M. F., Poole, R. J., Takayasu, D., Oshima, T., Konishi, J., Denda, K., and Masasuke, Y. (1989) *Proc. Natl. Acad. Sci. U. S. A.* **86,** 6661–6665
37. Iwabe, N., Kuma, K.-I., Hasegawa, M., Osawa, S., and Miyata, T. (1989 *Proc. Natl. Acad. Sci. U. S. A.* **86**, 9355–9359
38. Brown, J. R., and Doolittle, W. F. (1995) *Proc. Natl. Acad. Sci. U. S. A.* **92,** 2441–2445
39. Hensel, R., Zwickl, P., Fabry, S., Lang, J., and Palm, P. (1989) *Can. J. Microbiol.* **35,** 81–85
40. Cerff, R. (1995) *Tracing Biological Evolution in Protein & Gene Structures*, Elsevier Science Publishers B.V., Amsterdam
41. Brinkmann, H., and Martin, W. F. (1996) *Plant Mol. Biol.* **30,** 65–75
42. Hess, D., Krüger, K., Knappik, A., Palm, P., and Hensel, R. (1995) *Eur. J. Biochem.* **233,** 227–237
43. Keeling, P., and Doolittle, F. W. (1996) *Proc. Natl. Acad. Sci. U. S. A.* **94,** 1270–1275
44. Takahashi, K., and Weiner, H. (1980) *J. Biol. Chem.* **255,** 8206–8209
45. Bedino, S., and Testore, G. (1992) *Int. J. Biochem.* **24,** 1697–1704
46. Siebers, B., Wendisch, V. F., and Hensel, R. (1997) *Arch. Microbiol.* **168,** 120–127
47. König, H., Skorko, R., Zillig, W., and Reiter, W.-D. (1982) *Arch. Microbiol.* **132,** 297–303
48. Saitou, N., and Nei, M. (1987) *Mol. Biol. Evol.* **4,** 406–425
49. Kimura, M. (1983) *The Neutral Theory of Molecular Evolution*, Cambridge University Press, Cambridge